19 Cystic and Cavitary Lung Disorders

K. Nishimura, S. Oguri and H. Itoh

Introduction

A "cystic lesion" is a nonspecific term used to describe an area of decreased lung opacity identified radiologically (1–4). These lesions can be focal or multifocal, bilateral or sometimes unilateral. The lesion should be distinguished from air-trapping caused by pathologies of the bronchus or blood vessels, and from a decrease in opacity due to mosaic perfusion. According to the definition by Webb et al., a cystic airspace is a thin-walled (usually < 3 mm), well-circumscribed, air-containing lesion with a diameter of 1 cm or more, and must be visible on high resolution computed tomography (HRCT) (3,4). The definitions with respect to the size and wall thickness are arbitrary, and there has been no consensus on the differentiation of a cystic lesion from other pathologic lesions with decreased lung opacity, such as cavities.

Cystic airspaces are commonly seen in patients with histiocytosis X and lymphangioleiomyomatosis (LAM), but can also be observed in other diseases (4). Honeycombing can also result in cystic airspaces. The term "cyst" is sometimes used to describe the dilatated airways observed in patients with cystic bronchiectasis. However, it is not typically used to refer to low attenuation areas due to emphysema.

Pulmonary Histiocytosis X

Pulmonary histiocytosis X (HX) is also called pulmonary Langerhans' cell histiocytosis or eosinophilic granuloma of the lung. The histologic characteristics of the initial clinical stage are a peribronchial distribution of granulomatous nodules, accompanied by either Langerhans' histiocytes or eosinophilic infiltration, or both (5). At advanced stages, the cellular granulomas may become fibrous or may form cystic lesions of unknown cause (6,7).

Most patients are young or middle-aged adults, and present with nonspecific symptoms of their respiratory tract such as a cough or dyspnea (6–8). Approximately 20% of these patients also have a pneumothorax (9). Male patients are slightly more predominant, and over 90% are smokers, suggesting that smoking may be a cause of this disease (5,10). However, the symptoms usually develop only after several years of smoking, and do not correlate with the cumulative amount of smoking, in contrast to other smoking-related pulmonary disorders such as emphysema or lung cancer. Therefore there is probably an underlying reaction mechanism that causes this disease, and smoking merely triggers this reaction cascade.

Chest radiographs often reveal diffuse and non-specific infiltrates that are reticulonodular, reticular or small nodular. Therefore, HX is often categorized as an interstitial lung disease, but is best distinguished from idiopathic pulmonary fibrosis by its preferential distribution to the upper lung (Fig. 19.1). However, it is usually difficult to identify the cystic airspaces using chest X-rays alone.

Cavitating small nodular opacities and small cystic opacities are distinct features of HX that may be found by CT (Figs 19.1, 19.2) (11–14). In addition, there are small nodular opacities without cavities that tend toward a centrilobular distribution. Moore et al. reported 12 cases of cystic airspaces and 8 cases of small nodular opacities in 17 HX patients (11). Furthermore, Brauner et al. reported that 17 of 18 patients with HX showed thin-walled cysts, and 14 had small nodular opacities that were usually less than 1 cm in diameter (12). According to Grenier et al. in a study of 51 patients with HX, 47% had nodular opacities less than 3 mm in diameter, 45% had opacities ranging from 3 to 10 mm, and only 24% had opacities larger than 10 mm (14). The number of nodular opacities varied from one case to another, and this variability probably reflects the activity of the disease (11,12).

Small cystic opacities have been called thin- or thick-walled cysts, cystic airspaces or cavitated nodules (11,12). Grenier et al. reported that in 51 patients with HX, 88% showed thin-walled cysts (less than 2 mm) whereas 55% showed thick-walled cysts (more than 2 mm) (14). The pres-

M. Sperber (ed.), *Radiologic Diagnosis of Chest Disease*

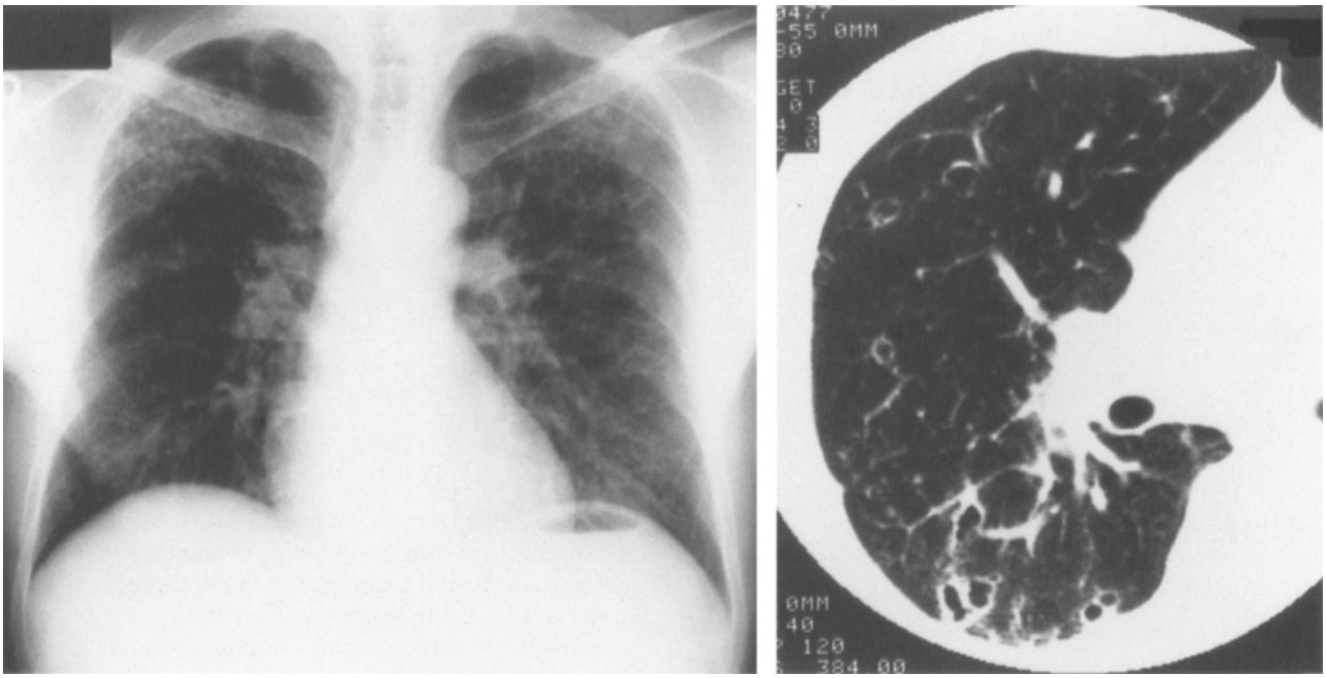

a b

Figure 19.1. Eosinophilic granuloma of the lung in a 44 year old male. **a** Posteroanterior chest radiograph shows reticulonodular infiltrates predominantly distributed in bilateral upper lungs. **b** CT scan with 5 mm collimation using targeted reconstruction in the same patient as in **a**, obtained at the same time, shows small cystic lesions with oval or lobulated shapes.

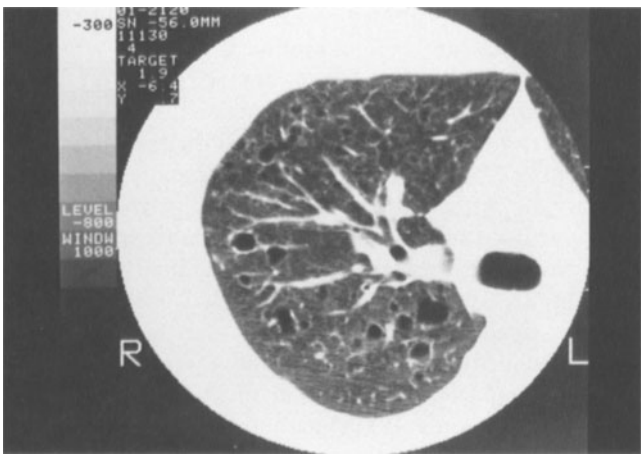

Figure 19.2. A 34 year old man with eosinophilic granuloma of the lung. CT scan with 5 mm collimation scan using targeted reconstruction shows thin-walled cystic airspaces.

ence of a distinct wall surrounding the cyst is useful in distinguishing HX from low attenuation areas due to emphysema. The cyst is usually circular in shape, but may manifest as bizarre shapes such as bilobed, clover-leaf shaped, or branched (11). These unusual shapes are generated by the fusion of several cysts, or occur sometimes because the cyst corresponds to a bronchus with dilatated, thin walls. The cysts tend to distribute preferentially to the upper lung, and the size of the cysts is usually larger in the upper lung as well. Cystic airspaces with these characteristics determined by HRCT strongly support the diagnosis of HX.

In many cases, the lung parenchyma between the cysts or nodules looks normal on CT scans, but irregular interfaces (interface sign), fine reticular opacities and ground-glass opacities may be observed in some cases (4). These appearances are usually indicative of intralobular fibrosis, early cyst formation and a confluence of cysts.

Based on a follow-up investigation using HRCT, these nodular opacities, thick-walled cysts and ground-glass opacities have been reported to regress with time. In contrast, the thin-walled cysts, linear opacities and emphysematous lesions either did not change or even progressed (15).

A comparative study of the CT appearance of these lesions with pulmonary function testing revealed a significant correlation between the diffusion capacity (DL_{co}) and the extent of the lesions. However, the extent of the airflow limitation did not correlate with the CT analysis (16). In addition, even in those cases where no airflow limitation was detected by the pulmonary function tests, an expiratory CT was able to demonstrate the presence of air-trapping and to indicate the presence of local airflow limitation (17).

Lymphangioleiomyomatosis

Lymphangioleiomyomatosis (LAM) is found only in premenopausal women, and can be characterized by the abnormal growth of atypical smooth muscle in the lung parenchyma and in the lymphatic vessels of the thorax and abdomen (18,19). The lung parenchyma develops

emphysematous lesions or thin-walled cysts via an unknown mechanism. It has been speculated that the growth of smooth muscle cells along the bronchioles may cause air-trapping. This growth of smooth muscle cells can also be observed in extrapulmonary lymph nodes such as the hilus and mediastinum, and results in an enlargement of the intrapulmonary lymphatics and thoracic duct, followed by chylous pleural effusion. Due to occlusion of the pulmonary vein, pulmonary hemorrhage can also be observed.

For most patients, the initial symptom is a shortness of breath, and 40% of these patients also present with pneumothorax. Chylous pleural effusion is also a common symptom, and hemosputum and hemoptysis are observed in 30–40% of the patients (19–25). LAM is only found in women who have pregnancy potential. Although there have been a few reports of LAM in postmenopausal women, these studies may not be trustworthy. Pregnancy can induce and often worsen LAM.

It appears to share some common features with the pulmonary involvement in patients with tuberous sclerosis. The relation of tuberous sclerosis with LAM has been debated. Renal angiomyolipomas are frequently found in patients with LAM.

The prognosis used to be quite unfavorable, but in recent years it has been reported that the 10 year survival rate was 20–40%, except for one study (20–22,23,26,27). There are some reports to support the therapeutic benefits of antiestrogen therapy, including an oophorectomy, but randomized controlled trials have not been performed. Therefore, there are still many questions about the effects of such treatments (23,26). Due to its progression, LAM is one disease in which lung transplantation has been performed.

Chest radiography in patients with LAM often does not show any specific features. There is usually an accompanying volume loss in interstitial lung disorders that are typical of diffuse infiltrative lung diseases. In contrast, LAM patients often develop hyperinflation instead. A complication such as a pneumothorax or chylous pleural effusion is often the key to identifying this disease.

The CT features of patients with LAM are characterized by numerous thin-walled cysts surrounded by a relatively normal lung parenchyma (Fig. 19.3) (28–36). The reported size of these cysts ranges from 2 to 50 mm, and the cysts grow bigger with the progress of the disease. The thickness of the cyst wall also ranges from what is barely detectable by HRCT to about 4 mm, but it tends to be thin. Typically, the cystic lesions are widely distributed throughout the entire lung, and there is no tendency toward a preferential distribution.

The majority of the lung parenchyma between the cysts is normal, but in some cases there may be a thickened interlobular septum, interstitial lesions or ground-glass opacities (4,18). The ground-glass opacity may correspond

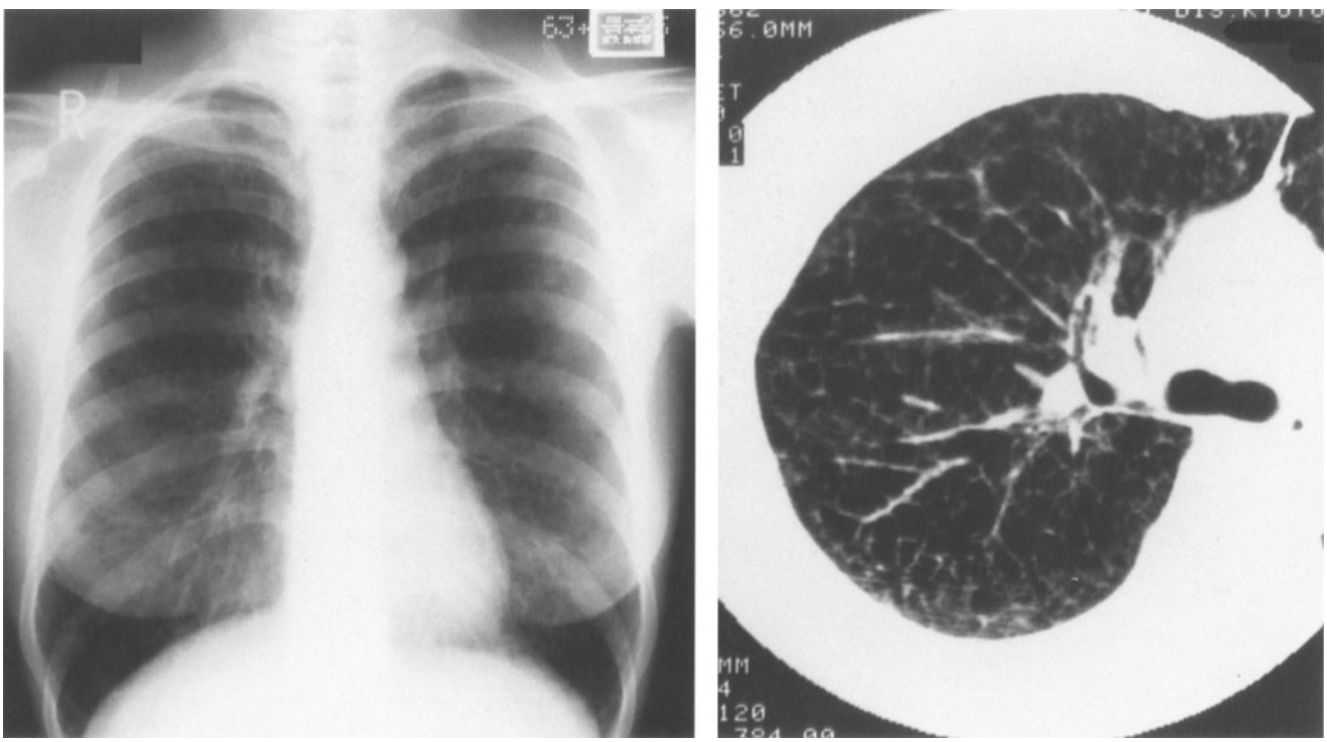

a b

Figure 19.3. A 37 year old female with lymphangioleiomyomatosis. She was almost a never smoker but had severe airflow limitation. **a** Posteroanterior chest radiograph shows hyperinflation associated with slightly increased vascular markings. **b** Targeted CT image through the right upper lung shows numerous low attenuation areas or small cystic abnormalities with or without thin walls.

to alveolar hemorrhage. On CT scans, there may also be enlargement of the hilar and mediastinal lymph nodes or pleural effusion. The former is believed to be due to the growth of smooth muscle cells in the lymph nodes, whereas the latter is thought to reflect chylous effusion.

A study examining the relationship between pulmonary function testing and the extent of the lesions observed on CT scans revealed that the diffusion capacity and airflow limitation correlated significantly with the extent of the disease observed by CT scans (34). In addition, when the LAM lesions in the lung are quantified using quantitative CT techniques, the CT index correlates significantly with physiologic measurements of the airflow, lung volume, diffusing capacity, and exercise performance, thus indicating the usefulness of a quantitative CT index for the evaluation of the disease severity (35). When examined using inspiratory CT, the size of the cysts was found to decrease upon expiration, indicating a communication between the cysts and the airway (17,36).

It is often an issue as to how to distinguish LAM from HX. Using CT images, the following three points are useful for differentiation: nodular components are often observed in HX, but are rare in LAM; irregularly shaped cysts are common in HX, but are rare in LAM; and HX lesions distribute preferentially to the upper lung and spare the costophrenic angle, whereas LAM lesions usually distribute diffusely over the whole lung.

It has been reported that micronodular pneumocyte hyperplasia is a rare manifestation of tuberous sclerosis or LAM. Although this is a histologic definition of multiple, well-demarcated nodules usually measuring up to 8 mm in size, micronodular pneumocyte hyperplasia should be considered if small nodular opacities are observed in patients with LAM (37).

Bronchiectasis

Reid morphologically classified bronchiectasis into three groups: saccular, varicose, and cylindrical. Reid's classification is the most commonly used, although saccular and varicose bronchiectases are sometimes combined and are termed cystic bronchiectasis. Cystic bronchiectasis ought to be distinguished from other cystic lesions in some cases. In particular, when there is an isolated cystic lesion on a section from CT scans, one must examine the continuity of the lesion to the proximal bronchus, and then judge whether it is bronchiectasis.

It is easy to diagnose cystic bronchiectasis by CT (Figs. 19.4, 19.5). However, for cylindrical bronchiectasis, it is sometimes difficult to determine the presence of dilatation. To diagnose bronchiectasis by CT, it is necessary to identify the bronchial wall because inflammatory thickening of the bronchial wall is an important factor for the diagnosis, along

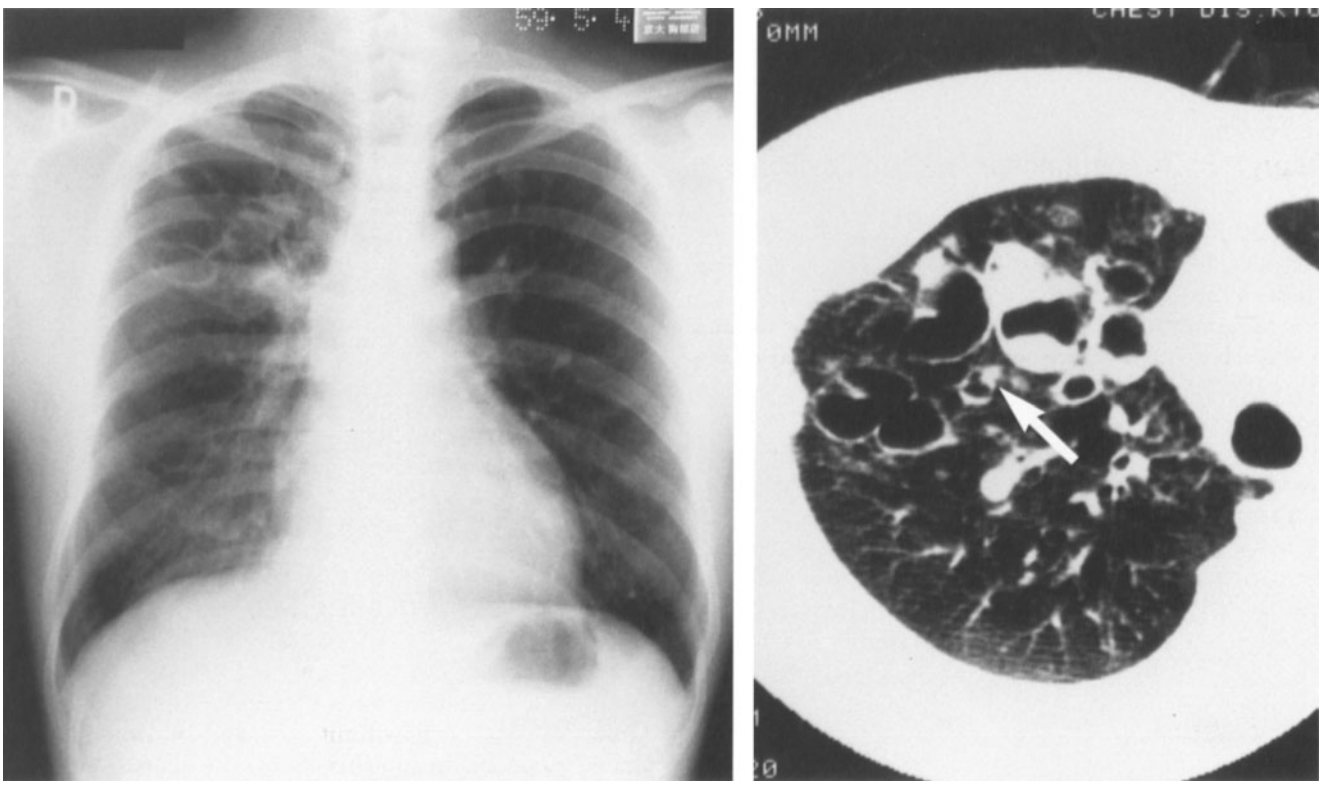

a b

Figure 19.4. Cystic bronchiectasis with unknown cause localized in right upper lobe in a 38 year old female. **a** Posteroanterior chest radiograph shows reticular or linear opacities in right upper lung. **b** CT scan with 5 mm collimation scan using a high spatial resolution algorithm shows markedly dilatated airways as well as signet-ring sign (*arrow*).

with dilatation of the airway. The "signet-ring sign" is frequently observed on CT scans from patients with bronchiectasis; this is a ring-shaped opacity (representing a dilatated, thick-walled airway) associated with a small, soft tissue opacity corresponding to the adjacent pulmonary artery (4).

Bronchography had been the most reliable method for making the diagnosis of bronchiectasis. In 1984, Müller et al examined 13 lungs and compared the diagnoses obtained by bronchography and CT (38). The CT diagnosis matched the bronchographic diagnosis in only 6 lungs. On the other hand, in 1985, Mootoosamy et al. examined bronchography versus CT in 36 lobes from 15 lungs, and demonstrated the usefulness of CT by matching all 22 positive and 14 negative diagnoses of bronchiectasis between these two techniques (39). In addition, Grenier et al. examined 44 lungs from 36 patients using bronchography and CT scans that were obtained at 1.5 mm collimation (40). They found that both techniques showed the same 25 as positive and the same 15 as negative. Bronchography has therefore been replaced by CT. The diagnostic power of CT compared with bronchography for determining bronchiectasis is approximately 55–100% for sensitivity and 92–100% for specificity (38–49). Therefore, there is a possibility that bronchiectasis may be missed using CT alone. Of course, a clear demonstration of bronchiectasis by CT will leave little need to perform bronchography (41).

Hansell et al. reported that patients with bronchiectasis frequently manifest air-trapping, even in those lobes that show no dilatation. Therefore, they speculated that the airway disease may precede the development of bronchiectasis (50).

Allergic Bronchopulmonary Aspergillosis (ABPA)

This is an allergic asthma caused by the growth of the fungus *Aspergillus* in the airway. The features of ABPA on chest radiographs are recurrent migratory infiltrates and central bronchiectasis. In addition, ABPA may also cause mucus plugging, airspace consolidation, and lobar or segmental collapse. Bronchiectasis is found more often in the proximal than in the distal airways, and consists mostly of a cystic or varicose dilatation. CT may detect the dilatation as an isolated cyst (4,51–54). The presence of central bronchiectasis is included in the secondary diagnostic criteria for ABPA. Expiratory CT scans have been reported to be useful for the detection of early-stage air-trapping, because it can sometimes detect air-trapping that cannot be detected during the inspiratory phase.

Cystic Fibrosis

This is an autosomal recessive genetic disorder found most frequently among Caucasians (55,56). Bronchiectasis and bronchial wall thickening are most frequently observed in patients with cystic fibrosis. These abnormalities can be easily detected by chest radiographs (57). The CT features include cystic or cylindrical bronchiectasis, bronchial wall thickening, mucus plugging, and hyperinflation (Fig. 19.5) (4,56–60).

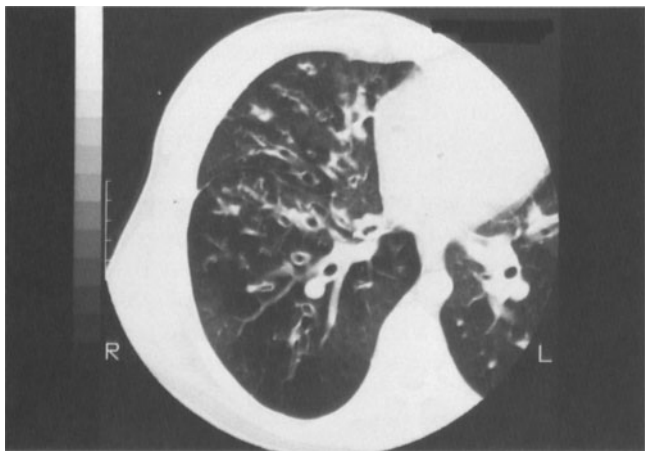

Figure 19.5. Cystic bronchiectasis in a 23 year old female patient with cystic fibrosis. HRCT scan with 2 mm collimation demonstrates cystic and cylindrical dilatation of bronchi and bronchial wall thickening. (Courtesy of Katashi Satoh and Satoko Hojo

Bronchiolitis Obliterans (BO)

BO is characterized by airflow limitation caused by the inflammation and fibrosis of the bronchioles. It has also been called constrictive bronchiolitis in recent years (61). It can be found with rheumatoid arthritis as well as with polymyositis/dermatomyositis, or it may be idiopathic. BO has also been reported as a manifestation of chronic rejection after lung or bone marrow transplantation (62). Hyperinflation is the most characteristic radiologic feature of BO, whereas the most frequent CT appearance is focal, decreased lung attenuation (4,62). This attenuated area contains pulmonary vessels with a decreased caliber. These changes correspond to the air-trapping or to the decrease in blood flow in the involved area; this is usually termed mosaic perfusion. It may manifest as either proximal or distal bronchiectasis. Expiratory CT has been reported to allow a clear demonstration of mosaic perfusion and air-trapping (36).

Diffuse Panbronchiolitis (DPB)

DPB is a unique disease found mainly in Asian countries (63,64). It is characterized by chronic respiratory tract infections and airflow limitation, and is always complicated by paranasal sinusitis (4,63). The histologic characterization of this disease is an interstitial accumulation of foamy macrophages in the respiratory bronchiolus, frequently accompanied by proximal bronchiectasis (65). The chest radiologic features include diffuse small

nodular infiltrates and hyperinflation (63). The main CT features are branching linear opacities and associated small nodular opacities; the latter show a centrilobular distribution (66). Akira et al. categorized the CT appearance of patients with DPB into four types, and type 4 indicates large cystic areas of high attenuation accompanied by dilatated proximal bronchi (67,68). Thus they showed that cystic lesions develop as the DPB progresses, and are an essentially irreversible phenomenon. In addition, although rare, there have been reports of DPB-like bronchiolitis lesions as a human T-cell lymphotrophic virus type 1 (HTLV-1) related bronchopulmonary disease found in carriers of the adult T-cell leukemia virus (69).

Honeycombing

Honeycombing is defined as the macroscopic appearance of bronchiolectasis surrounded by fibrous lesions (70,71). It is generally viewed as the nonspecific, final stage of pulmonary fibrosis, and is therefore sometimes called an "end-stage" lung (72). Honeycomb cystic airspaces range from a few millimeters to several centimeter in diameter, and are characterized by clearly definable walls which can be thick. The cystic airspaces of the honeycomb tend to share walls. The mechanism and process of chronic honeycombing formation is almost unknown.

Coarse reticular shadows on chest radiographs often correspond to honeycombing (73). The superiority of CT over chest radiography as a detection method for honeycombing is well known. On CT scans, aggregates of cysts that are thick walled, bigger than 2 mm in diameter, and relatively similar in size indicate honeycombing. The spaces between the dilatated bronchioles consist of fibrous lesions instead of air-containing alveoli. Therefore the cysts are in contact with each other through a thick wall. Such aggregates of small cysts are typical, but are difficult to observe even using HRCT when the honeycombing consists of cysts less than 1 mm in diameter. In this case, mildly dilatated airways can be observed in a high-attenuation area (air bronchiologram-like appearance) (70). This latter feature is sometimes difficult to distinguish from lesions with airspace consolidation. The details of diffuse infiltrative lung disorders are discussed in Chapter 19.

Usual interstitial pneumonia (UIP) is the major lung pathology of idiopathic pulmonary fibrosis (IPF) or cryptogenic fibrosing alveolitis (74). It is also the most common pathologic pattern in the pulmonary involvement of various collagen-vascular diseases. The frequency of UIP in the pulmonary involvement of various collagen-vascular diseases depends on the type of disease (75,76).

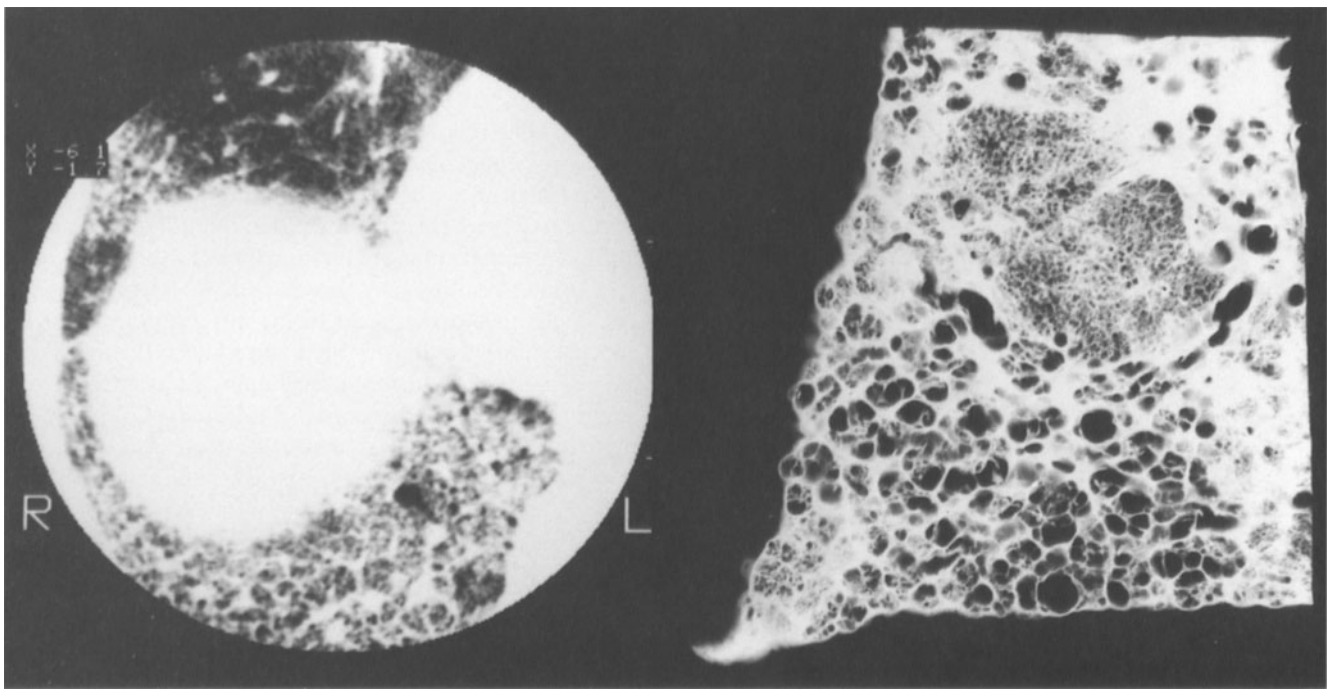

a b

Figure 19.6. Macroscopic honeycombing in UIP. **a** CT in a 65 year old man, through the right lung base, demonstrates accumulated cystic spaces with thick walls. Since the patient died of exacerbation of idiopathic pulmonary fibrosis an autopsy was performed 36 days after this CT scan was performed. **b** Contact radiograph of the postmortem right lower lung, fixed using Heitzman's solution. The gross honeycombing corresponded to the accumulated cystic spaces with thick walls seen at CT scan. The histologic examination of the postmortem lungs revealed both UIP and diffuse alveolar damage.

For example, the pulmonary involvement of systemic sclerosis is thought to be almost always UIP (76). An important feature for the histologic diagnosis of UIP is that both the normal alveolar areas and the areas of fibrosis are observed in the same tissue specimen (secondary pulmonary lobule), with a patchy distribution (77). The fibrous lesions may begin at the alveolar septum, but there is no clear explanation on how they develop to the final stage of fibrosis and honeycombing. Since there are aggregates of alveoli in the wall of the honeycomb, the regions affected by the honeycombing also show a decrease in volume. Honeycombing is found at a very high frequency in UIP, but such lesions do not have any histologic value for making the diagnosis (Fig. 19.6) (70,78–82).

The various effects of smoking on IPF have been studied (83,84). When smokers develop IPF, any dysfunction that should otherwise be revealed by pulmonary function testing could be masked or modified. Histologically, this modification indicates the copresence of pulmonary emphysema caused by smoking and pulmonary fibrosis. The chest radiologic findings may reveal isolated or interspersed cystic lesions that are not continuous with the honeycombing. Such cysts are often distributed to the upper lungs, and are categorized as emphysema or emphysematous bullae. On CT scans, pulmonary emphysema is described as low attenuation areas without walls. However, because of the fibrous lesions in the surrounding area, pulmonary emphysema may appear like a cyst with a wall.

The long-term prognosis of *pulmonary sarcoidosis* is relatively favorable. Honeycombing is found only in a small proportion of patients with sarcoidosis (85–87). Sarcoidosis is discussed in Chapter 15.

Pulmonary histiocytosis X or *eosinophilic granuloma of the lung* is a disease with a generally favorable prognosis. However, in some cases, the fibrosis worsens and results in death. Since it is a relatively rare disease, the mortality rate of this disease is not known. A centrilobular fibrosis is believed to be important in this case. Since the lesions may distribute over the entire lung at advanced stages, it is often difficult to diagnose this disease even using CT.

The pulmonary lesions of *asbestosis* also show honeycombing, and its CT features are discussed in Chapter 26. In most cases, *desquamative interstitial pneumonia (DIP)* and *lymphocytic interstitial pneumonia (LIP)* do not show any honeycombing upon biopsy. However, honeycombing may develop later and can be detected by CT.

Acute interstitial pneumonia (AIP) is an interstitial pneumonia that shows a relatively acute progression, and has neither any preceding pulmonary lesions nor any obvious extrapulmonary cause (88,89). Clinically, similar histologic features have been recognized as the final state of the lung on the autopsies of patients diagnosed with adult respiratory distress syndrome (ARDS) or other extensive lung diseases; these features are pathologically categorized as those belonging to diffuse alveolar damage (DAD), or acute lung injury (90). Ground-glass opacities accompanied by a volume loss are recognized on chest radiographs of most cases showing histologic lesions characteristic of DAD. The stage showing microscopic honeycomb formation corresponds histologically to organized DAD, and CT scans reveal air bronchiologram-like distal airways inside the high attenuation areas (70). However, this feature on the CT scans is not enough to diagnose the presence of microscopic honeycombing by itself (89). The honeycombing caused by DAD stays at the microscopic level, and usually does not grow to macroscopic honeycombing.

Emphysema

Emphysema is defined histologically as permanent, abnormal enlargement of the airspaces distal to the terminal bronchiole, which is accompanied by the destruction of the walls of the involved alveoli, but is not associated with any obvious fibrosis (91). On the basis of localization of these lesions in the secondary pulmonary lobule, emphysema can be categorized as follows: centrilobular or centriacinar emphysema, panacinar or panlobular emphysema, and paraseptal or distal acinar emphysema. The radiological appearance of emphysema is discussed in Chapter 17.

Centrilobular emphysema is found preferentially in the upper lung, and appears on CT scans as a small, low attenuation area without any obvious walls (92–96). In contrast, low attenuation areas may not been clearly observed in panlobular emphysema even using CT, and thus a mild lesion of this type is more difficult to recognize than centrilobular emphysema (97). Paraseptal emphysema can be recognized as small subpleural cysts or bullae. Some patients with emphysema show multiple bullae on CT scans, and the walls of these cysts may or may not be clearly recognizable, but in either case it is termed bullous emphysema (Fig. 19.7). It is often difficult to determine the relative contribution of the parenchymal emphysema and the bullae to the overall pulmonary dysfunction. It is also often difficult to determine the indications for the surgical resection of the bullae.

Infective Lung Disorders with Cavitary or Cystic Lesions

Pulmonary Tuberculosis

Tuberculosis is one of the most frequent pulmonary infectious diseases that cause cavitating lesions. Pulmonary tuberculosis is usually categorized into either primary pulmonary tuberculosis or reactivation tuberculosis.

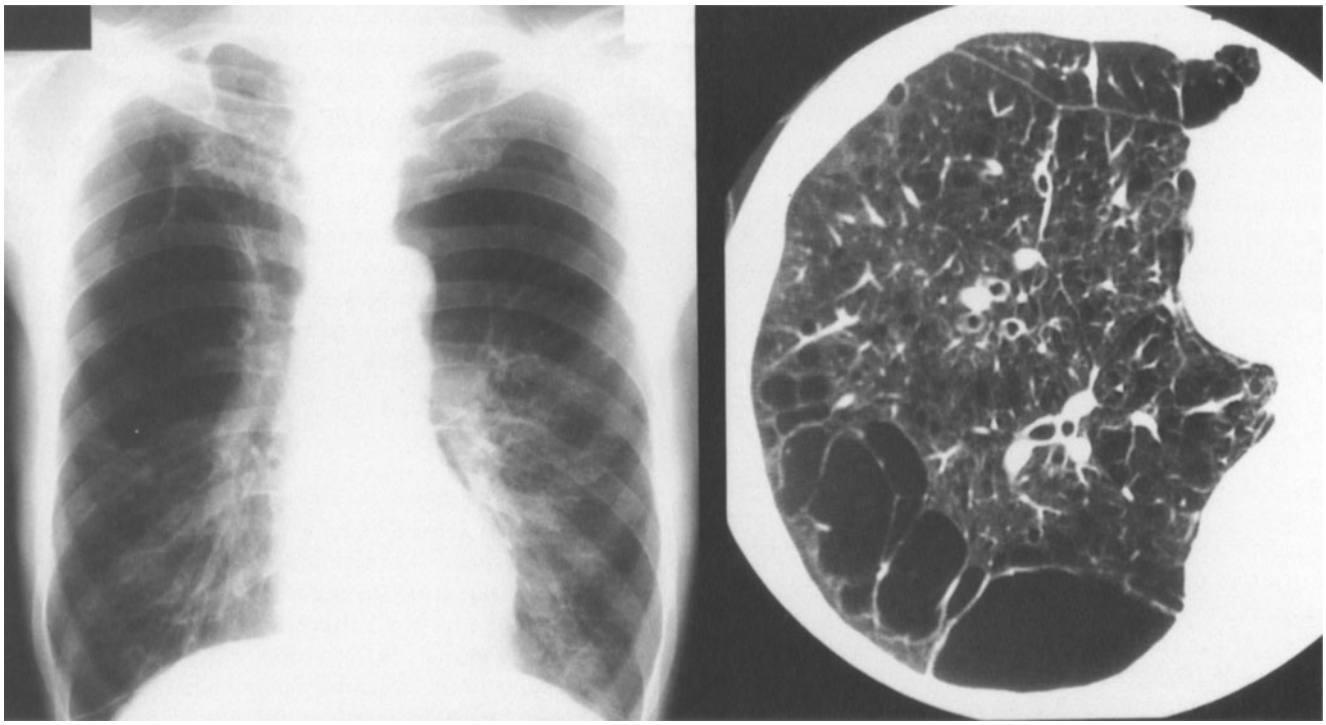

a b

Figure 19.7. Bullous emphysema in a 67 year old male. He was a former smoker with moderate airflow limitation. Forced expiratory volume in one second (FEV_1) was 1.14 L (41% predicted). **a** Posteroanterior chest radiograph shows hyperinflation. **b** Targeted CT image with 2 mm collimation through the right lower lung demonstrates low attenuation areas corresponding to emphysema associated with several cystic airspaces.

Previously, it has been believed that tuberculous pleuritis or miliary tuberculosis follows the primary complex. These concepts ought to be reexamined, since the aged population now often experiences miliary or pleural tuberculosis. The radiological appearance of pulmonary tuberculosis is discussed in Chapter 14.

The radiologic features of primary tuberculosis are airspace consolidation, lobar or segmental collapse, and hilar or mediastinal lymphadenopathy. Cavitation has been reported in 29% of tuberculosis patients (98). Many cases of tuberculosis, which is recognized as a community-acquired disease at many clinics daily, are actually reactivation tuberculosis; its roentgenographic features are summarized by focal consolidation and cavitation observed at the apex or upper lobe. It is most important to suspect tuberculosis based on the chest radiologic features and to look for acid-fast bacilli in the sputum. Of course, it is best to obtain the diagnosis prior to conducting a CT scan. However, in recent years, there have been an increasing number of reports on the CT features of pulmonary tuberculosis (99–107).

Webb et al. summarized the HRCT findings of active tuberculosis as follows: patchy unilateral or bilateral airspace consolidation frequently peribronchial in distribution, thin- or thick-walled cavitation, scattered airspace nodules, and the superimposition of centrilobular branching structures (4). Im and colleagues reported that cavitating nodules were found as a HRCT feature in 69% of 41 patients with active pulmonary tuberculosis (103). Most of these cavities were thick walled, but thin-walled cavities are often seen as well in patients undergoing, and after treatment. In pulmonary tuberculosis, it has been generally thought that there is no special relationship between the CT features of these lesions and their activity. Nevertheless, antituberculous chemotherapy usually helps the cavities to resolve. In addition, CT is useful for the diagnosis of mycetoma (fungus ball), which often complicates the cavitating lesions, especially after treatment for tuberculosis.

Nontuberculous (Atypical) Mycobacterial Infections

Although there are regional differences in the incidence and type of nontuberculous mycobacterial infections, *Mycobacterium avium intracellular complex* (MAC) and *Mycobacterium kansasii* are the two most common pathogens that cause lung lesions (108). There have been several reports on the CT features of in nonimmunocompromised patients and human immunodeficiency virus (HIV)-infected hosts with MAC-related pulmonary disease (108–115), which manifests radiographic features

very similar to those tuberculosis (109,110). However, some authors concluded that there were prominent features indicative of widespread bronchiectasis, particularly if it involves the right middle lobe and lingula (114,115). Cavities, small nodular opacities and airspace consolidation are also frequently observed on CT scans.

Pneumocystis Carinii Pneumonia (PCP)

Immunocompromised patients, especially HIV-infected patients, are highly susceptible to PCP, and the infiltrates often spread to bilateral lungs (116–119). The characteristic CT features of PCP are ground-glass opacities and airspace consolidation that distribute preferentially from the hilus to the internal layers of the lung, with a "patchwork" or "mosaic" pattern (4,117). The "patchwork" distribution pattern of these lesions is unique for this disease, and less involved areas are present between the lesions. Another characteristic is the presence of thick-walled, irregular, and septated cavities or thin-walled cysts (119). There have also been some reports on the relationship between cyst formation and a pneumothorax (120). The fact that the cysts are found preferentially in the upper lobe, together with other reports, indicates that about 35% of PCP cases result in cyst formation. Bronchiectasis is also frequently observed in patients with PCP using CT (121). PCP is further discussed in Chapter 18.

Septic Embolism and Infarction

Septic pulmonary embolisms and infarctions are observed in patients with sepsis or in patients with a intravenous fixed catheter. When there are multiple nodules at varying stages of cavitation, it should be considered as a differential diagnosis. On CT scans, they show nodular or wedge-shaped triangular opacities at the peripheral regions of the lung, especially in the subpleural areas, and these lesions are often accompanied by cavitation with thick walls (122, 123). The nodular lesions may also manifest feeding vessels.

Invasive Pulmonary Aspergillosis

Invasive pulmonary aspergillosis is a pneumonia caused by *Aspergillus*. This pathogen infects only immunocompromised patients, in contrast to the other two pulmonary diseases which are caused by *Aspergillus* and occur in nonimmunocompromised patients, i.e. aspergilloma and allergic bronchopulmonary aspergillosis. It is an opportunistic infection, and those immunocompromised patients who have a hematologic malignancy such as leukemia are the most susceptible.

Aspergillus has a tendency to invade the pulmonary vessels, and therefore frequently causes hemosputum or hemoptysis. Invasive aspergillosis causes diffuse or focal airspace consolidation, nodules, and cavitating lesions (124–127). A relatively characteristic feature of invasive aspergillosis on CT is the halo sign, which is a ground-glass opacity surrounding a nodule (124). Pathologically, this feature corresponds to coagulation necrosis or hemorrhaging in the area surrounding the nodules. It has been reported that thick-walled, cavitating lesions are the most common radiologic manifestation of invasive aspergillosis in acquired immune deficiency syndrome (AIDS) (126).

Pulmonary Cryptococcosis

Pulmonary Cryptococcosis can be categorized into the following two types; a community-acquired disease in non-immunocompromised patients, and an opportunistic cryptococcus infection in patients with HIV infection or in other immunocompromised hosts (128–130). These fungal infections have great regional variability in the world, and thus one must be aware of the regional frequency and pathology for its differential diagnosis.

Nonimmunocompromised patients with pulmonary cryptococcosis manifest no or only mild symptoms (130). The chest radiographic features include focal or multiple nodular opacities, whereas CT scans reveal nodules with cavities at a higher frequency (Fig. 19.8). These nodules are concentrated in a relatively limited area, but can distribute diffusely to bilateral lungs. They are often found in the subpleural region, may sometimes accompany pleural indentation with irregular edges, and may need to be differentiated from an adenocarcinoma of the lung. Many reports on the CT features of this disease are cases of pulmonary cryptococcosis as a complication of AIDS. About 30% of the pulmonary cryptococcosis cases in AIDS patients manifest nodules that have been observed at an early stage of the HIV infection. Adenopathy or pleural effusion may sometimes be seen as well. Atypical, miliary nodules or ground-glass opacities can also be observed, and in these cases it may be necessary to distinguish it from PCP.

Other Fungal Diseases

Pulmonary nocardiosis is a subacute or chronic lung infection caused by *Nocardia asteroides*. Nocardiosis can be found in nonimmunocompromised hosts, but more often in immunocompromised patients with lymphomas as well as AIDS. In addition, it is known to occur as a complication of pulmonary alveolar proteinosis, pulmonary tuberculosis, and chronic granulomatous diseases. There

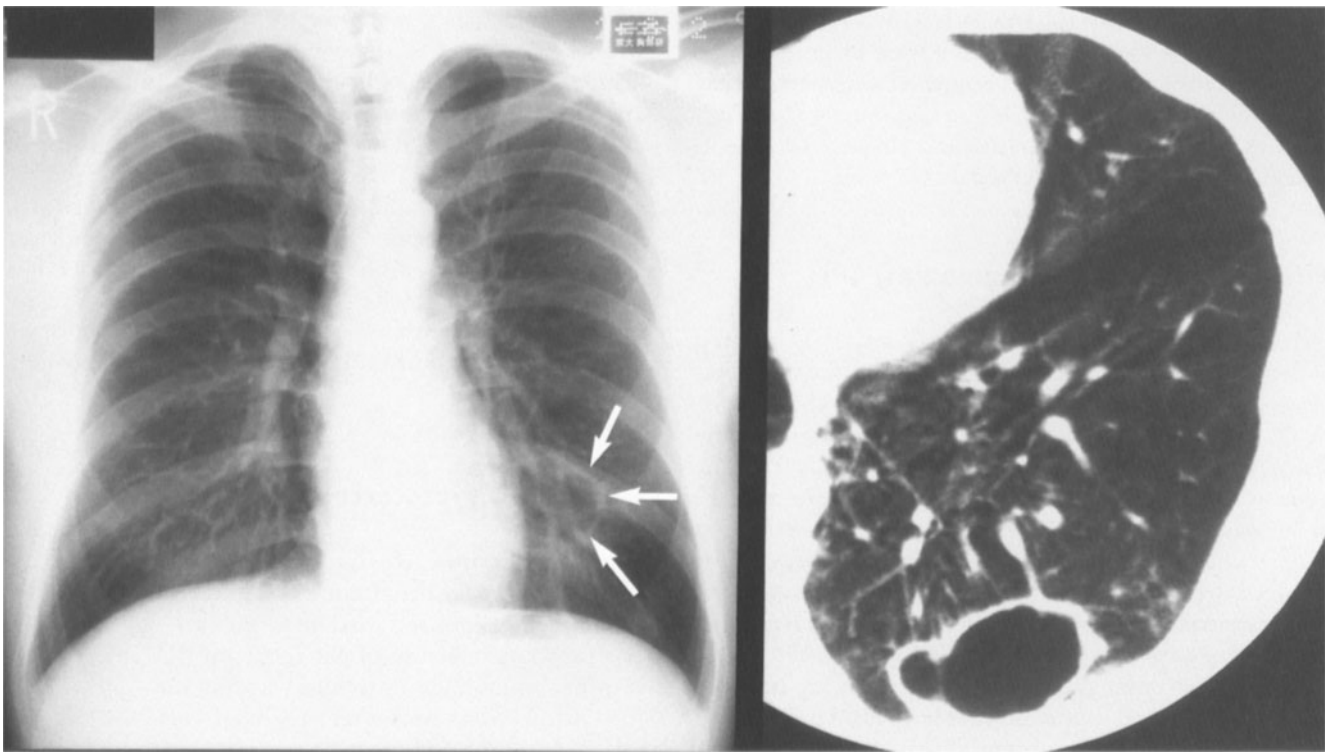

a b

Figure 19.8. Pulmonary cryptoccocosis without evidence of dissemination in a 27 year old asymptomatic nonimmunocompromised male patient. **a** Posteroanterior chest radiograph shows single cystic space (*arrows*) located in the inner zones of the left lower lung. **b** Targeted CT image through the left lower lung demonstrates solitary large cyst with wall thickness of about 5 mm, located in 10th segment of the left lung.

are only a limited number of reports on its radiologic appearance, but diffuse infiltration and multiple nodules as well as cavitation are commonly observed.

Cavitation is also a common feature of coccidioidomycosis and histoplasmosis, and is occasionally observed in blastomycosis, actinomycosis, and sporotrichosis. Cavitating pneumonia is also seen in immunocompromised patients with invasive candidiasis.

Lung Abscess

The lung abscesses or chronic pneumonia caused by *Staphylococcus, Legionella*, and Gram-negative bacilli including *Klebsiella* occasionally undergo necrosis and cavity formation. Cavitation is also common for hematogenous lung abscesses. The radiologic appearance of lung abscesses is discussed in Chapter 22.

Parasitic Cavity

Hydatid cysts of the lung are occasionally associated with cavitary formation. Multiple small cavities can be seen in patients with paragonimiasis, and amebic lung abscesses have been reported in patients with hepatic amoebiasis.

Noninfectious Granulomatous Lung Diseases

The chest radiologic features of *Wegener granulomatosis* are parenchymal opacification, nodular opacities, bronchial and pleural abnormalities (131–136). Bilateral or unilateral nodular opacities of various sizes are clearly observed on CT scans, and are accompanied by cavities in about 50% of the cases (131,132). The walls of the cavitating lesions are usually thick. Some nodules demonstrate an angiocentric or bronchocentric distribution on CT scans. Wedge-shaped nodular opacities adjacent to the pleura are a common feature, and pleural effusion is also frequently observed. For laboratory findings, antineutrophil cytoplasmic autoantibody specific for antiproteinase 3 (c-ANCA) is useful for a diagnosis of Wegener granulomatosis.

The pathologic characteristics of *pulmonary sarcoidosis* include a perilymphatic distribution of noncaseating granuloma. The characteristic feature on CT scans is

peribronchovascular small nodules (86,87). Airspace consolidation as well as large nodules with diameters greater than 1 cm can also be observed on CT scans. Such large nodules may be cavitated in rare cases (86). Grenier et al. reported that these large cavitated nodules were found in 3% of patients with pulmonary sarcoidosis (14). There are also reports describing cases of pulmonary sarcoidosis which presented as bullous emphysema with severe airflow limitation (137).

Neoplasmatic Cavitation

Lung Cancer and Metastatic Carcinoma

Regardless of the histologic diagnosis, lung cancers can manifest cavity formation, possibly due to necrosis of the central region of the tumor. In squamous cell carcinomas, cavities with thick walls are often formed. In addition, the cancers can grow inside bullae or along the walls, and can show features resembling cavitary formation on chest radiographs and CT. It has been reported that cystic airspaces are observed within lobar or diffuse consolidation on the CT scans of patients with bronchioloalveolar carcinoma (138). There is often cavity or cystic formation inside the multiple nodular opacities caused by metastases from malignant tumors (Fig. 19.9).

Lymphoproliferative or Lymphoinfiltrative Lung Disorders

Lymphoproliferative or lymphoinfiltrative lung disorders include various diseases, from highly malignant ones such as malignant lymphoma to those that are currently considered to be benign. On the basis of several characteristic histologic features, there are a number of terms used to describe diseases with diffuse or local lymphoproliferative or lymphoinfiltrative lung involvement: lymphoid interstitial pneumonia, pseudolymphoma, lymphomatoid granulomatosis, plasma cell granuloma, mucosa-associated lymphoid tissue lymphoma (MALTOMA), and multicentric Castlemann disease. Furthermore, lymphoproliferative or lymphoinfiltrative lung disorders have been reported as the lung manifestation of Sjögren syndrome and AIDS (Fig. 19.10). Gene analysis is currently considered to be a valuable technique in determining whether the lymphoid hyperplasia is related to a tumor.

Cavitation is less common in patients with non-Hodgkin lymphoma than in those with Hodgkin disease. However, the cavitation of pulmonary nodules is rather rare in patients with non-Hodgkin lymphoma (139,140). The lung lesions of multicentric Castlemann disease also manifest cystic formation at high frequency in addition to centrilobular ill-defined nodules, thickening of the bronchovascular bundles and interlobular septal thickening (141). In addition, CT appearance of lymphocytic interstitial pneumonia may show ground-glass attenuation, airspace consolidation, ill-defined nodules and cysts (142).

Pulmonary Sequestration

Pulmonary sequestration is defined as the supply of blood from the systemic circulation to a part of the lung where there is no communication with a normal bronchus. There are two types of pulmonary sequestra-

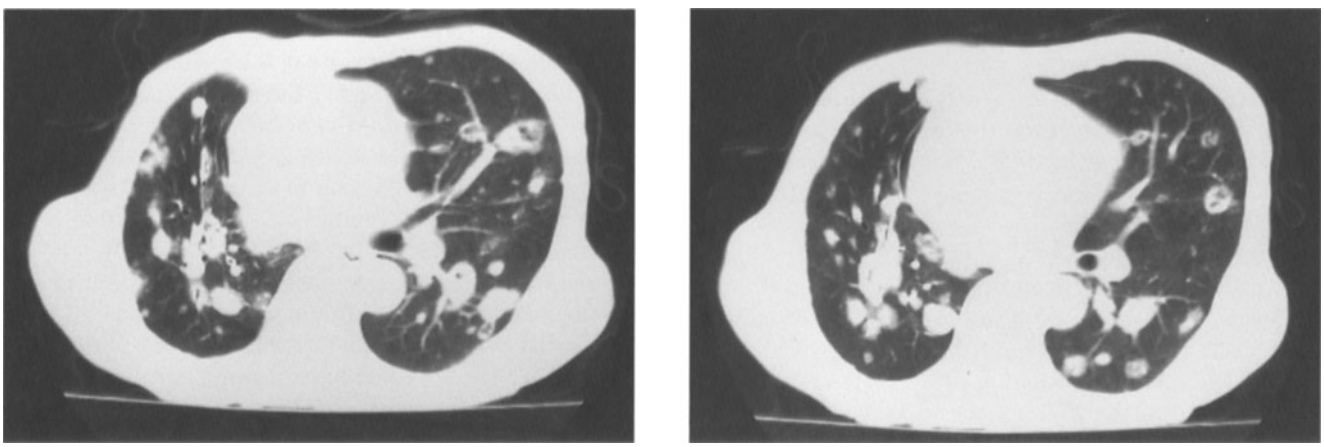

a b

Figure 19.9. Postoperative recurrence of adenocarcinoma of lung. Multiple cavitary nodules are demonstrated at CT scans in a 73 year old female who underwent right upper lobectomy 10 years prior to the scan.

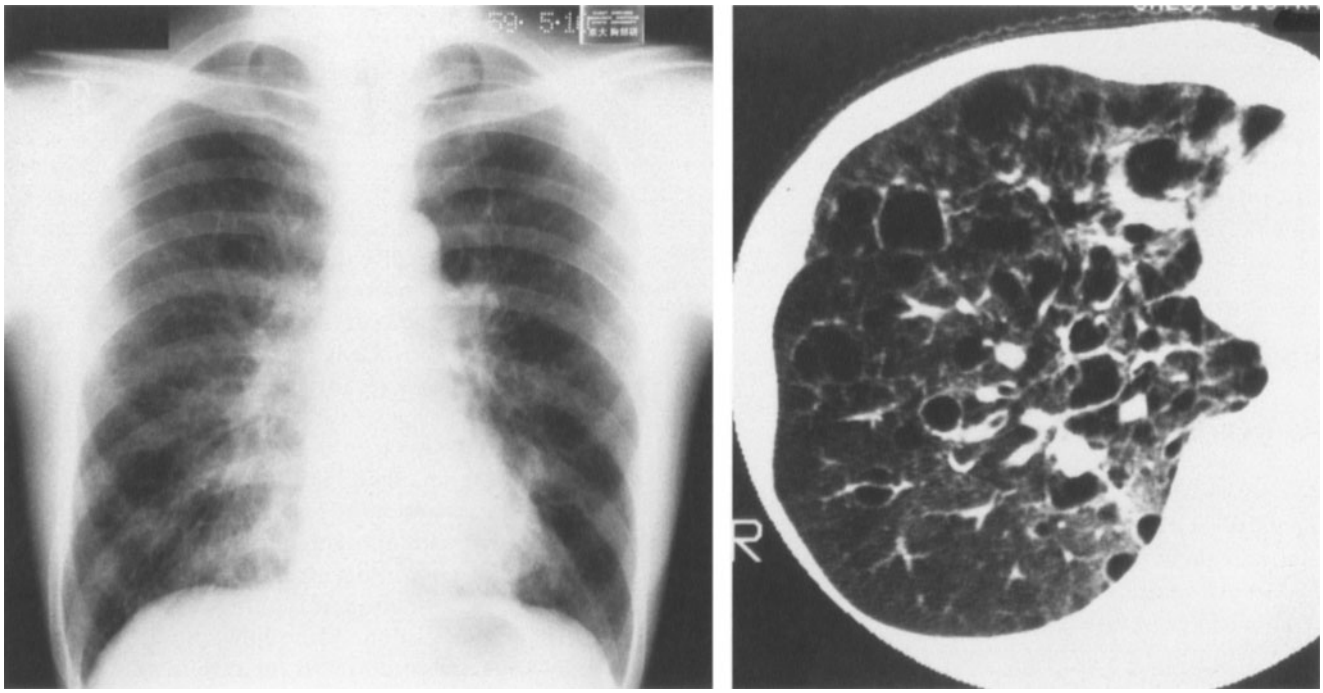

a b

Figure 19.10. Lymphoproliferative lung disorders associated with Sjögren's syndrome in a 44 year old male. **a** Posteroanterior chest radiograph shows ground-glass opacities predominantly distributed in the inner zones of bilateral lower lungs and mild hyperinflation. **b** Targeted CT image through the right lower lung demonstrates several cystic airspaces with a variety of wall thickness.

tion: intralobar pulmonary sequestration, which shares a pleura with the normal lung; and extralobar pulmonary sequestration, which is enclosed in an independent pleura.

About 75% of pulmonary sequestration is intralobar. Since there is no pleura between the sequestration and the normal lung, it can often result in infection via an acquired communication with the bronchi. Therefore, cystic airspaces are frequently observed in intralobar pulmonary sequestration. The sequestration develops almost exclusively in the posterior basal segment (S10) of the left lower lobe (Fig. 19.11). Blood flows into the sequestration through an artery branching from the aorta, and flows out into the pulmonary veins. On the other hand, extralobar pulmonary sequestration is less prone to infection because it is surrounded by a layer of visceral pleura.

Without infection, the sequestration is seen as a homogeneous tumor adjacent to the left diaphragm. Complications with infection result in the formation of multiple cystic lesions, and sometimes the presence of air–fluid levels. Therefore the formation of multiple cysts is more frequent in intralobar pulmonary sequestration. Thoracic aortography provides the definitive diagnosis, but contrast CT may also reveal abnormal blood vessels branching from the aorta.

Mediastinal Cysts and Other Extrapulmonary Lesions

Most mediastinal cysts are congenital in origin, and these cysts comprise about 9% of the mediastinal mass in an adult. The radiologic appearance of mediastinal tumors and cysts is discussed in Chapter 34.

Bronchogenic cysts are the most common, and appear on CT scans as circular or oval shapes with smooth edges. The walls are too thin to recognize. Bronchogenic cysts can be observed anywhere along the mediastinum, but are often found in the middle to posterior mediastinum.

The CT features of *esophageal duplication cysts* are similar to those of bronchogenic cysts, and therefore these two types of cyst are difficult to distinguish. Sixty percent of esophageal cysts are found in the lower portion of the posterior mediastinum (143).

Pericardial cysts are thin-walled sacs formed during the development of the pericardium. They are connected at the pericardial cavity via the funiculus, but there is no communication. Those cysts that have a communication with the lumen of the pericardial cysts are called pericardial cyst diverticuli. In 90% of these cases, the cysts are in contact with the diaphragm. In 65% and 25% of these cases, they are found at the right and left cardiophrenic angles, respectively.

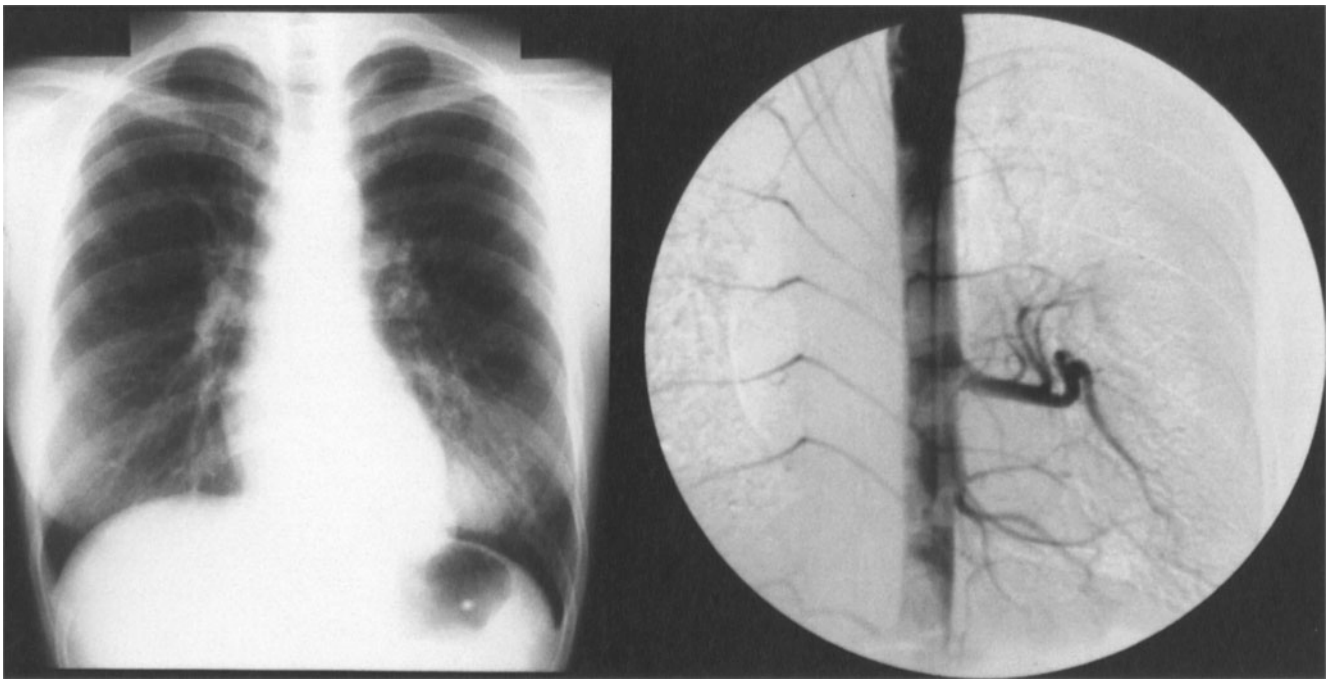

a b

Figure 19.11. Intralobar pulmonary sequestration in a 23 year old female. **a** Posteroanterior chest radiograph shows mass-like opacity in left lower lung, but cystic abnormality is not evident in this case. **b** Thoracic aortography demonstrates feeding artery originating from descending aorta. Surgical procedure proved her to be having intralobar pulmonary sequestration.

Patients with a *pneumothorax*, a *pneumomediastinum*, or a diaphragmatic hernia show intrathoracic air that can be easily diagnosed by CT scans.

References

1. Tuddenham WJ (1984) Glossary of terms for thoracic radiology: Recommendations of the Nomenclature Committee of the Fleischner Society. AJR 143:509–517.
2. Lillington GA (1987) A diagnostic approach to chest diseses. Differential diagnosis based on roentgenographic patterns, 3rd edn. Williams & Wilkins, Baltimore, MD.
3. Webb WR, Müller NL, Naidich DP (1993) Standardized terms for high-resolution computed tomography of the lung: A proposed glossary. J Thorac Imaging 8:167–175.
4. Webb WR, Müller NL, Naidich DP (1996) High-resolution CT of the lung, 2nd edn. Lippincott-Raven Publishers, Philadelphia.
5. Travis WD, Borok Z, Roum JH, et al. (1993) Pulmonary Langerhans' cell granulomatosis (histiocytosis X). A clinicopathologic study of 48 cases. Am J Surg Pathol 17:971–986.
6. Colby TV, Lombard C (1983) Histiocytosis X in the lung. Hum Pathol 14:847–856.
7. Marcy TW, Reynolds HY (1985) Pulmonary histiocytosis X. Lung 163:129–150.
8. Schünfeld N, Frank W, Wenig S, et al. (1993) Clinical and radiologic features, lung function and therapeutic results in pulmonary histiocytosis X. Respiration 60:38–40.
9. Lewis JG (1964) Eosinophilic granuloma and its variants with special reference to lung involvemet: A report of 12 patients. Q J Med 33:337–359.
10. Mogulkoc N, Veral A, Bishop PW, et al. (1999) Pulmonary Langerhans' cell histiocytosis. Radiologic resolution following smoking cessation. Chest 115:1452–1455.
11. Moore ADA, Godwin JD, Müller NL, et al. (1989) Pulmonary histiocytosis X: Comparison of radiographic and CT findings. Radiology 172:249–254.
12. Brauner MW, Grenier P, Mouelhi MM, et al. (1989) Pulmonary histiocytosis X: Evaluation with high-resolution CT. Radiology 172:255–258.
13. Kulwiec EL, Lynch DA, Aguayo SM, et al. (1992) Imaging of pulmonary histiocytosis X. Radiographics 12:515–526.
14. Grenier P, Valeyre D, Cluzel P, et al. (1991) Chronic diffuse interstitial lung disease: Diagnostic value of chest radiography and high-resolution CT. Radiology 179:123–132.
15. Brauner MW, Grenier P, Tijani K, et al. (1997) Pulmonary Langerhans' cell histiocytosis: Evolution of lesions on CT scans. Radiology 204:497–502.
16. Kelkel E, Pison C, Brambilla E, et al. (1992) Value of high resolution tomodensitometry in pulmonary histiocytosis X: Radiological, clinical and functional correlations. Rev Mal Respir 9:307–311.
17. Stern EJ, Webb WR, Golden JA, et al. (1992) Cystic lung disease associated with eosinophilic granuloma and tuberous sclerosis: air trapping at dynamic ultrafast high-resolution CT. Radiology 182:325–329.
18. Corrin B, Liebow AA, Friedman PJ (1975) Pulmonary lymphangioleiomyomatosis. A review. Am J Pathol 79:347–382.
19. Carrington CB, Cugell DW, Gaensler EA, et al. (1977) Lymphangioleiomyomatosis: Physiologic–pathologic–radiologic correlations. Am Rev Respir Dis 116:977–995.
20. Taylor JR, Ryu J, Colby TV, et al. (1990) Lymphangioleiomyomatosis. Clinical course in 32 patients. N Engl J Med 323:1254–1260.

21. Kitaichi M, Nishimura K, Itoh H, et al. (1995) Pulmonary lymphangioleiomyomatosis: A report of 46 patients including a clinicopathologic study of prognostic factors. Am J Respir Crit Care Med 151:527–533.
22. Sullivan EJ (1998) Lymphangioleiomyomatosis. A review. Chest 114:1689–1703.
23. Moss J, Ross R, Vaughan M, et al. (1999) Report of workshop on lymphangioleiomyomatosis. Am J Respir Crit Care Med 159:679–683.
24. Oh YM, Mo EK, Jang SH, et al. (1999) Pulmonary lymphangioleiomyomatosis in Korea. Thorax 54:618–621.
25. Chu SC, Horiba K, Usuki J, et al. (1999) Comprehensive evaluation of 35 patients with lymphangioleiomyomatosis. Chest 115: 1041–1052.
26. Krishna G, Berry G, Kao P, et al. (1999) Update on the treatment of lymphangioleiomyomatosis. Clin Pulm Med 6:126–132.
27. Johnson SR, Tattersfield AE (1999) Decline in lung function in lymphangioleiomyomatosis. Relation to menopause and progesterone treatment. Am J Respir Crit Care Med 160:628–633.
28. Merchant RN, Pearson MG, Rankin RN, et al. WKC (1985) Computerized tomography in the diagnosis of lymphangioleiomyomatosis. Am Rev Respir Dis 131:295–297.
29. Rappaport DC, Weisbrod GL, Herman SJ, et al. DW (1989) Pulmonary lymphangioleimyomatosis: High-resolution CT findings in four cases. AJR 152:961–964.
30. Sherrier RH, Chiles C, Roggli V (1989) Pulmonary lymphangioleiomyomatosis: CT findings. AJR 153:937–940.
31. Templeton PA, McLoud TC, Müller NL, et al. (1989) Pulmonary lymphangioleiomyomasosis: CT and pathologic findings. J Comput Assist Tomogr 13:54–57.
32. Lenoir S, Grenier P, Brauner MW, et al. (1990) Pulmonary lymphangiomyomatosis and tuberous sclerosis: Comparison of radiographic and thin-section CT findings. Radiology 175:329–334.
33. Müller NL, Chiles C, Kullnig P (1990) Pulmonary lymphangiomyomatosis: Correlation of CT with radiographic and functional findings. Radiology 175:335–339.
34. Aberle DR, Hansell DM, Brown K, et al. (1990) Lymphangiomyomatosis: CT, chest radiographic, and functional correlations. Radiology 176:381–387.
35. Crausman RS, Lynch DA, Mortenson RL, et al. (1996) Quantitative CT predicts the severity of physiologic dysfunction in patients with lymphangioleiomyomatosis. Chest 109:131–137.
36. Worthy SA, Brown MJ, Müller NL (1998) Technical report: Cystic air spaces in the lung: Change in size on expiratory high-resolution CT in 23 patients. Clin Radiol 53:515–519.
37. Muir TE, Leslie KO, Popper H, et al. (1998) Micronodular pneumocyte hyperplasia. Am J Surg Pathol 22:465–472.
38. Müller NL, Bergin CJ, Ostrow DN, et al. (1984) Role of computed tomography in the recognition of bronchiectasis. AJR 143:971–976.
39. Mootoosamy IM, Reznek RH, Osman J, et al. (1985) Assessment of bronchiectasis by computed tomography. Thorax 40:920–924.
40. Grenier P, Maurice F, Musset D, et al. (1986) Bronchiectasis: Assessment by thin-section CT. Radiology 161:95–99.
41. Pang JA, Hamilton-Wood C, Metreweli C (1989) The value of computed tomography in the diagnosis and management of bronchiectasis. Clin Radiol 40:40–44.
42. Young K, Aspestrand F, Kolbenstvedt A (1991) High resolution CT and bronchography in the assessment of bronchiectasis. Acta Radiologica 32:439–441.
43. Marti-Bonmati L, Catala FJ, Ruiz Perales F (1991) Computed tomography differentiation between cystic bronchiectasis and bullae. J Thorac Imaging 7:83–85.
44. Kang EY, Miller RR, Müller NL (1995) Bronchiectasis: Comparison of preoperative thin-section CT and pathologic findings in resected specimens. Radiology 195:649–654.
45. van der Bruggen-Bogaarts BAHA, van der Bruggen HMJG, van Waes PFGM, et al. (1996) Screening for bronchiectasis. A comparative study between chest radiography and high-resolution CT. Chest 109:608–611.
46. Smith IE, Jurriaans E, Diederich S, et al. (1996) Chronic sputum production: Correlations between clinical features and findings on high resolution computed tomographic scanning of the chest. Thorax 51:914–918.
47. King MA, Stone JA, Diaz PT, et al. (1996) α1-Antitrypsin deficiency: Evaluation of bronchiectasis with CT. Radiology 199:137–141.
48. Lucidarme O, Grenier P, Coche E, et al. (1996) Bronchiectasis: Comparative assessment with thin-section CT and helical CT. Radiology 200:673–679.
49. Miszkiel KA, Wells AU, Rubens MB, et al. (1997) Effects of airway infection by Pseudomonas aeruginosa: A computed tomographic study. Thorax 52:260–264.
50. Hansell DM, Well AU, Rubens MB, et al. (1994) Bronchiectasis: Functional significance of areas of decreased attenuation at expiratory CT. Radiology 193:369–374.
51. Currie DC, Goldman JM, Cole PJ, et al. (1987) Comparison of narrow section computed tomography and plain chest radiography in chronic allergic bronchopulmonary aspergillosis. Clin Radiol 38:593–596.
52. Kullning P, Pongratz M, Kopp W, et al. (1989) Computerized tomography in the diagnosis of allergic bronchopulmonary aspergillosis. Radiology 29:228–231.
53. Neeld DA, Goodman LR, Gurney JW, et al. (1990) Computerized tomography in the evaluation of allergic bronchopulmonary aspergillosis. Am Rev Respir Dis 142:1200–1205.
54. Panchal N, Bhagat R, Pant C, et al. (1997) Allergic bronchopulmonary aspergillosis: The spectrum of computed tomography appearances. Respir Med 91:213–219.
55. Hojo S, Fujita J, Obayashi Y, et al. (1997) Two cases of cystic fibrosis in Japanese/German twins. Jap J Thorac Dis 35:1259–1264.
56. Hojo S, Fujita J, Miyawaki H, et al. (1998) Severe cystic fibrosis associated with ΔF508/R347H+D979A compound heterozygous genotype. Clin Genet 53:50–53.
57. Friedman PJ (1987) Chest radiologic findings in the adult with cystic fibrosis. Semin Roentgenol 22:114–124.
58. Hansell DM, Strickland B (1989) High-resolution computed tomography in pulmonary cystic fibrosis. Br J Radiol 62:1–5.
59. Santis G, Hodson ME, Strickland B (1991) High resolution computed tomography in adult cystic fibrosis patients with mild lung disease. Clin Radiol 44:20–22.
60. Taccone A, Romano L, Marzoli A, et al. (1991) Computerized tomography in pulmonary cystic fibrosis. Radiol Med 82:79–83.
61. Kraft M, Mortenson RL, Colby TV, et al. (1993) Cryptogenic constrictive bronchiolitis. A clinicopathologic study. Am Rev Respir Dis 148:1093–1101.
62. Morrish WF, Herman SJ, Weisbrod GL, et al. (1991) Bronchiolitis obliterans after lung transplantation: findings at chest radiography and high-resolution CT. Radiology 179:487–490.
63. Homma H, Yamanaka A, Tanimoto S, et al. (1983) Diffuse panbronchiolitis. A disease of the transitional zone of the lung. Chest 83:63–69.
64. Randhawa P, Hoagland MH, Yousem SA (1991) Diffuse panbronchiolitis in North America. Report of three cases and review of the literature. Am J Surg Pathol 15:43–47.
65. Kitaichi M, Nishimura K, Izumi T (1991) Diffuse panbronchiolotis. In Sharma OP (ed) Lung diseases in the Tropics. Marcel Dekker, Inc., New York, pp 479–509.
66. Nishimura K, Kitaichi M, Izumi T, et al. (1992) Diffuse panbronchiolitis: Correlation of high-resolution CT and pathologic findings. Radiology 184:779–785.

67. Akira M, Kitatani F, Yong-Sik L, et al. (1988) Diffuse panbronchiolitis: Evaluation with high-resolution CT. Radiology 168:433–438.
68. Akira M, Higashihara T, Sakatani M (1993) Diffuse panbronchiolitis: Follow-up CT examination. Radiology 189:559–562.
69. Sugimoto M, Kitaichi M, Ikeda A, et al. (1998) Chronic bronchiolo-alveolitis associated with human T-cell lymphotrophic virus type 1 infection. Curr Opin Pulm Med 4:98–102.
70. Nishimura K, Kitaichi M, Izumi T, et al. (1992) Usual interstitial pneumonia: Histologic correlation with high-resolution CT. Radiology 182:337–342.
71. Itoh H, Murata K, Konishi J, et al. (1993) Diffuse lung disease: Pathologic basis for the high-resolution computed tomography findings. J Thorac Imaging 8:176–188.
72. Westcott JL, Cole SR (1986) Traction bronchiectasis in end-stage pulmonary fibrosis. Radiology 161:665–669.
73. Heitzman ER (1984) The Lung. Radiologic–pathologic correlations, 2nd edn. Mosby, St. Louis. MO.
74. Crystal RG, Fulmer JD, Roberts WC, et al. (1976) Idiopathic pulmonary fibrosis: Clinical, histologic, radiographic, physiologic, scintigraphic, cytologic, and biochemical, aspects. Ann Intern Med 85:769–788.
75. Yousem SA, Colby TV, Carrington CB (1985) Lung biopsy in rheumatoid arthritis. Am Rev Respir Dis 131:770–777.
76. Chan TYK, Hansell DM, Rubens MB, et al. (1997) Cryptogenic fibrosing alveolitis and the fibrosing alveolitis of systemic sclerosis: Morphological differences on computed tomographic scans. Thorax 52:265–270.
77. Carrington CB, Gaensler EA, Coutu RE, et al. (1978) Natural history and treated course of usual and desquamative interstitial pneumonia. N Engl J Med 298:801–809.
78. Akira M, Sakatani M, Ueda E (1993) Idiopathic pulmonary fibrosis: Progression of honeycombing at thin-section CT. Radiology 189:687–691.
79. Wells AU, Rubens MB, du Bois RM, Hansell DM (1993) Serial CT in fibrosing alveolitis: Prognostic significance of the initial pattern. AJR 161:1159–1165.
80. Mino M, Noma S, Kobashi Y, et al. (1995) Serial changes of cystic air spaces in fibrosing alveolitis: a CT–pathological study. Clin Radiol 50:357–363.
81. Hartman TE, Primack SL, Kang EY, et al. (1996) Disease progression in usual interstitial pneumonia compared with desquamative interstitial pneumonia. Assessment with serial CT. Chest 110:378–382.
82. Lee JS, Gong G, Song KS, et al. (1998) Usual interstitial pneumonia: Relationship between disease activity and the progression of honeycombing at thin-section computed tomography. J Thorac Imaging 13:199–203.
83. Wiggins J, Strickland B, Turner-Warwick M (1990) Combined cryptogenic fibrosing alveolitis and emphysema: The value of high resolution computed tomography in assessment. Respir Med 84:365–369.
84. Hanley ME, King TE, Jr., Schwarz MI, et al. (1991) The impact of smoking on mechanical properties of the lungs in idiopathic pulmonary fibrosis and sarcoidosis. Am Rev Respir Dis 144:1102–1106.
85. Hiraga Y, Yamamoto M, Tachibana T, et al. (1981) Pulmonary fibrosis in severe pulmonary sarcoidosis. In Mikami R, Hosoda Y (eds) Sarcoidosis. University of Tokyo Press, Tokyo, pp 291–300.
86. Nishimura K, Itoh H, Kitaichi M, et al. (1993) Pulmonary sarcoidosis: Correlation of CT and histopathologic findings. Radiology 189:105–109.
87. Nishimura K, Itoh H, Kitaichi M, et al. (1995) CT and pathologic correlation of pulmonary sarcoidosis. Semin Ultrasound, CT MR 16:361–370.
88. Katzenstein ALA, Myers JL, Mazur MT (1986) Acute interstitial pneumonia: A clinicopathologic, ultrastructural and cell kinetic study. Am J Surg Pathol 10:256–267.
89. Primack SL, Hartman TE, Ikezoe J, et al. (1993) Acute interstitial pneumonia: Radiographic and CT findings in nine patients. Radiology 188:817–820.
90. Katenstein AA, Bloor CM, Leibow AA (1976) Diffuse alveolar damage – the role of oxygen, shock, and related factors. A review. Am J Pathol 85:210–228.
91. Snider GL, Kleinerman J, Thurlbeck WM (1985) The definition of emphysema. Report of a National Heart, Lung, and Blood Institute, Division of Lung Diseases Workshop Report. Am Rev Respir Dis 132:182–185.
92. Bergin C, Müller NL, Nichols DM, et al. (1986) The diagnosis of emphysema. A computed tomographic–pathologic correlation. Am Rev Respir Dis 133:541–546.
93. Foster WL, Jr, Pratt PC, Roggli VL, et al. (1986) Centrilobular emphysema: CT-pathologic correlation. Radiology 159:27–32.
94. Hruban RH, Meziane MA, Zerhouni EA, et al. (1987) High resolution computed tomography of inflation-fixed lungs. Pathologic–radiologic correlation of centrilobular emphysema. Am Rev Respir Dis 136:935–940.
95. Miller RR, Müller NL, Vedal S, et al. (1989) Limitations of computed tomography in the assessment of emphysema. Am Rev Respir Dis 139:980–983.
96. Kuwano K, Matsuba K, Ikeda T, et al. (1990) The diagnosis of mild emphysema. Correlation of computed tomography and pathology scores. Am Rev Respir Dis 141:169–178.
97. Spouge D, Mayo JR, Cardoso W, et al. (1993) Panacinar emphysema: CT and pathologic findings. J Comput Assist Tomogr 17:710–713.
98. Woodring JH, Vandiviere HM, Fried AM, et al. (1986) Update: The radiographic features of pulmonary tuberculosis. AJR 146:497–506.
99. Kuhlman JE, Deutsch JH, Fishman EK, et al. (1990) CT features of thoracic mycobacterial disease. Radiographics 10:413–431.
100. Hill AR, Premkumar S, Brustein S, et al. (1991) Disseminated tuberculosis in the acquired immunodeficiency syndrome era. Am Rev Respir Dis 144:1164–1170.
101. Ikezoe J, Takeuchi N, Johkoh T, et al. (1992) CT appearance of pulmonary tuberculosis in diabetic and immunocompromised patients: Comparison with patients who had no underlying disease. AJR 159:1175–1179.
102. Tsao TCY, Juang YC, Tsai YH, et al. (1992) Whole lung tuberculosis. A disease with high mortality which is frequently misdiagnosed. Chest 101:1309–1311.
103. Im JG, Itoh H, Shim YS, et al. (1993) Pulmonary tuberculosis: CT findings – early active disease and sequential change with antituberculous therapy. Radiology 186:653–660.
104. Leung AN, Brauner MW, Gamsu G, et al. (1996) Pulmonary tuberculosis: Comparison of CT findings in HIV-seropositive and HIV-seronegative patients. Radiology 198:687–691.
105. Hatipoglu ON, Osma E, Manisali M, et al. (1996) High resolution computed tomographic findings in pulmonary tuberculosis. Thorax 51:397–402.
106. Lee KS, Hwang JW, Chung MP, et al. (1996) Utility of CT in the evaluation of pulmonary tuberculosis in patients without AIDS. Chest 110:977–984.
107. Poey C, Verhaegen F, Giron J, et al. (1997) High resolution chest CT in tuberculosis: Evolutive patterns and signs of activity. J Comput Assist Tomogr 21:601–607.
108. Miller WT Jr, Miller WT (1993) Pulmonary infections with atypical mycobacteria in the normal host. Semin Roentgenol 28:139–149.
109. Primack SL, Logan PM, Hartman TE, et al. (1995) Pulmonary tuberculosis and Mycobacterium avium-intracellulare: A comparison of CT findings Radiology 194:413–417.
110. Laissy JP, Cadi M, Cinqualbre A, et al. (1997) Mycobacterium tuberculosis versus nontuberculous mycobacterial infection of the

lung in AIDS patients: CT and HRCT patterns. J Comput Assist Tomogr 21:312–317.
111. Hartman TE, Swensen SJ, Williams DE (1993) Mycobacterium avium-intracellulare complex: Evaluation with CT. Radiology 187:23–26.
112. Moore EH (1993) Atypical mycobacterial infection in the lung: CT appearance. Radiology 187:777–782.
113. Swensen SJ, Hartman TE, Williams DE (1994) Computed tomographic diagnosis of Mycobacterium avium-intracellulare complex in patients with bronchiectasis. Chest 105:49–52.
114. Lynch DA, Simone PM, Fox MA, et al. (1995) CT features of pulmonary Mycobacterium avium complex infection. J Comput Assist Tomogr 19:353–360.
115. Obayashi Y, Fujita J, Suemitsu I, et al. (1999) Successive follow-up of chest computed tomography in patients with Mycobacterium avium-intracellulare complex. Respir Med 93:11–15.
116. Hartman TE, Primack SL, Müller NL, et al. (1994) Diagnosis of thoracic complication in AIDS: Accuracy of CT. AJR 162:547–553.
117. Kuhlman JE, Kavuru M, Fishman EK, et al. (1990) Pneumocystis carinii pneumonia: Spectrum of parenchymal CT findings. Radiology 175:711–714.
118. Bergin CJ, Wirth RL, Berry GJ, et al. (1990) Pneumocystis carinii pneumonia: CT and HRCT observations. J Comput Assist Tomogr 14:756–759.
119. Chow C, Templeton PA, White CS (1993) Lung cysts associated with Pneumocystis carinii pneumonia: Radiographic characteristics, natural history, and complications. AJR 161:527–531.
120. Goodman PC, Daley C, Minagi H (1986) Spontaneous pneumothorax in AIDS patients with Pneumocystis carinii pneumonia. AJR 147:29–31.
121. McGuinness G, Naidich DP, Garay SM, et al. (1993) AIDS associated bronchiectasis: CT features. J Comput Assist Tomogr 17:260–266.
122. Kuhlman JE, Fishman EK, Teigen C (1990) Pulmonary septic emboli: Diagnosis with CT. Radiology 174:211–213.
123. Balakrishnan J, Meziane MA, Siegelman SS, et al. (1989) Pulmonary infarction: CT appearance with pathologic correlation. J Comput Assist Tomogr 13:941–945.
124. Hruban RH, Meziance MA, Zerhouni EA, et al. (1987) Radiologic–pathologic correlation of the CT halo sign in invasive pulmonary aspergillosis. J Comput Assist Tomogr 11:534–536.
125. Logan PM, Primack SL, Miller RR, et al. (1994) Invasive aspergillosis of the airways: Radiographic, CT, and pathologic findings. Radiology 193:383–388.
126. Staples CA, Kang EY, Wright JL, et al. (1995) Invasive pulmonary aspergillosis in AIDS: Radiographic, CT, and pathplogic findings. Radiology 196:409–414.
127. Won HJ, Lee KS, Cheon JE, et al. (1998) Invasive pulmonary aspergillosis: prediction at thin-section CT in patients with neutropenia – a prospective study. Radiology 208:777–782.
128. Patz EF Jr, Goodman PC (1992) Pulmonary cryptococcosis. J Thorac Imaging 7:51–55.
129. Lee LN, Yang PC, Kuo SH, et al. (1993) Diagnosis of pulmonary cryptococcosis by ultrasound guided percutaneous aspiration. Thorax 48:75–78.
130. Aberg JA, Mundy LM, Powderly WG (1999) Pulmonary cryptococcosis in patients without HIV infection. Chest 115:734–740.
131. Cordier JF, Valeyre D, Guillevin L, et al. (1990) Pulmonary Wegener's granulomatosis. A clinical and imaging study of 77 cases. Chest 97:906–912.
132. Kuhlman JE, Hruban RH, Fishman EK (1991) Wegener granulomatosis: CT features of parenchymal lung disease. J Compt Assist Tomogr 15:948–952.
133. Weir IH, Müller NL, Chiles C, et al. (1992) Wegener's granulomatosis: findings from computed tomography of the chest in 10 patients. Can Assoc Radiol J 43:31–34.
134. Maskell GF, Lockwood CM, Flower CDR (1993) Computed tomography of the lung in Wegener's granulomatosis. Clin Radiol 48:377–380.
135. Reuter M, Schnabel A, Wesner F, et al. (1998) Pulmonary Wegener's granulomatosis. Correlation between high-resolution CT findings and clinical scoring of disease activity. Chest 114:500–506.
136. Attali P, Begum R, Ban-Romdhane H, et al. (1998) Pulmonary Wegener's granulomatosis: Changes at follow-up CT. Eur Radiol 8:1009–1113.
137. Judson MA, Strange C (1998) Bullous sarcoidosis. A report of three cases. Chest 114:1474–1478.
138. Trigaux JP, Gevenosis PA, Goncette L, et al. (1996) Bronchioloalveolar carcinoma: Computed tomography findings. Eur Respir J 9:11–16.
139. Cordier JF, Chailleux E, Lauque D, et al. (1993) Primary pulmonary lymphomas. A clinical study of 70 cases in nonimmunocompromised patients. Chest 103:201–208.
140. Jackson SA, Tung KT, Mead GM (1994) Multiple cavitating pulmonary lesions in non-Hodgkin's lymphoma. Clin Radiol 49:883–885.
141. Johkoh T, Müller NL, Ichikado K, et al. (1998) Intrathoracic multicentric Castleman disease: CT findings in 12 patients. Radiology 209:477–481.
142. Ichikawa Y, Kinoshita M, Koga T, et al. (1994) Lung cyst formation in lymphocytic interstitial pneumonia: CT features. J Comput Assist Tomogr 18:745–748.
143. Macpherson RI (1993) Gastrointestinal tract duplications: Clinical, pathologic, etiologic, and radiologic considerations. Radiographics 13:1063–1080